HHS Public Access

Author manuscript

Pulm Pharmacol Ther. Author manuscript; available in PMC 2017 August 01.

Published in final edited form as:

Pulm Pharmacol Ther. 2016 August ; 39: 64–73. doi:10.1016/j.pupt.2016.06.004.

Targeted drug delivery to emphysematous lungs: Inhibition of MMPs by doxycycline loaded nanoparticles

Vaideesh Parasaram[1], **Nasim Nosoudi**[1], **Renee J LeClair, Ph.D**[2], **Andrew Binks, Ph.D**[2], and **Naren Vyavahare, Ph.D**[1,$]

[1]Department of Bioengineering, Clemson University, SC

[2]University of South Carolina School of Medicine, Greenville, SC

Graphical Abstract

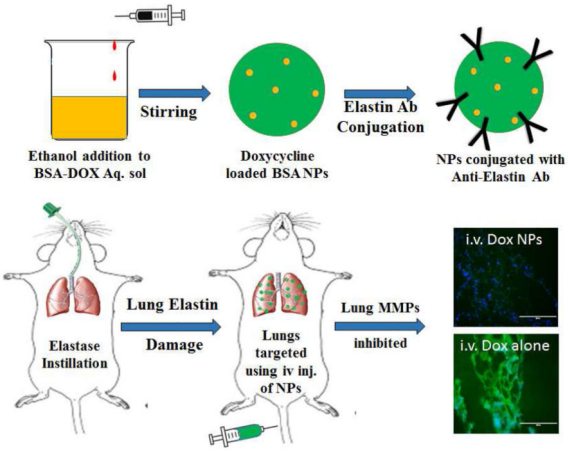

1. Introduction

Chronic obstructive pulmonary disease (COPD) is the third leading cause of death in U.S. following cancer and heart disease. Current hypothesis regarding mechanism of emphysema suggest that chronic exposure to cigarette smoke and particulate matter causes irritation in the alveoli and this triggers an inflammatory response. This response attracts a host of inflammatory cells like macrophages, neutrophils, and lymphocytes. Cytokines, reactive oxygen species, prostaglandins, leukotrienes, proteases mediate the progression of the disease [1, 2].

Of particular interest to this research is emphysema in COPD patients. This results in poorly reversible airway obstruction due to the destruction of alveoli and elastin fibers in the lung

[$]Corresponding Author: 501 Rhodes Research Center, Clemson University, SC, 29634, narenv@clemson.edu, Telephone: 864-656-5558.

[3, 4]. Loss of elastin in the lungs correlates to loss of lung function in patients [5, 6]. Currently available treatments for COPD aim at only providing temporary relief to the patients by mitigating inflammation or by the action of bronchodilators [7–10]. Corticosteroids have been shown to have no anti-inflammatory effect in COPD patients [11]. None of the available treatments has shown promising effect on treating the disease yet.

Matrix metalloproteinases (MMPs) have received a lot of attention in emphysema research with their key role in damaging elastin fibers, thus contributing to the enlargement of air spaces and loss of elastic recoil in the lungs [12]. Use of MMP inhibitors in COPD has been explored in animal models [13, 14] but there is always the risk of off-targeting of MMPs with the systemic delivery of these drugs [15]. Doxycycline is one potential broad-spectrum MMP inhibitor. It is the only FDA approved MMP inhibitor that is widely available. It is shown to inhibit early inflammation in diseases like pulmonary fibrosis [16, 17] by reducing MMP activity in smooth muscle cells [18, 19]. It can also be used as a treatment for COPD exacerbations.

While the exact process of MMP inhibition by doxycycline (or tetracyclines in general) is not known, it is believed that this happens by both direct inhibition of MMPs and by inhibiting their expression. Direct inhibition involves chelation of bivalent ions like Ca^{2+} or Zn^{2+} which are essential for the functioning of these enzymes [20]. Liu et al., [18] observed reduced MMP-2 mRNA half life but steady state MMP-2 mRNA production by human smooth muscle cells (SMCs) *in vitro*, there by proposing a post-transcriptional destabilization of MMP-2 mRNA by doxycycline. Additionally, doxycycline specifically targets endothelial cells where it inhibits MMP synthesis [21].

Nanoparticles have recently been investigated as potential drug delivery systems to the lungs because of various advantages they offer [22]. In order to increase the specificity and availability of nanoparticles loaded with drugs, use of monoclonal antibodies to specific biomolecules within the lungs has been suggested as a potential opportunity but has been poorly explored [23, 24]. Inhalation of drug-loaded particulates via aerosols is common way to deliver drugs to the lungs. However, inhalation of drugs to treat pulmonary disorders has certain limitations. The fate of an inhaled particle depends on its size, anatomy of airways and ventilatory parameters [25–27]. Despite the plethora of drug delivery opportunities available, there is a greater need for a highly effective delivery method, which combines an active targeting formulation and consistent local release of a drug for enhanced therapeutic effect.

In this paper, we investigated a novel method of drug delivery, in a rat elastase model of emphysema, with a systemic injection of nanoparticles loaded with doxycycline, an MMP inhibitor. We took advantage of elastin damage in emphysema and tested our hypothesis that anti-elastin coated bovine serum albumin (BSA) nanoparticles injected intravenously will target the lungs and will release doxycycline over a period to suppress MMP activity in lungs.

2. Materials and Methods

2.1. Preparation of DiR loaded nanoparticles (DiR-BSA NPs)

DiR (1, 1-dioctadecyl-3, 3, 3, 3-tetramethylindotricarbocyanine iodide) (PromoCell GmbH, Heidelberg, Germany) loaded bovine serum albumin (BSA) (Seracare, Milford, MA) nanoparticles were prepared as described previously [28]. These particles were PEGylated (Maleimide-PEG NHS ester) (Avanti Polar Lipids, Inc., Alabaster, AL) and conjugated to anti-elastin antibody as described previously [29]. DiR dye was loaded to track the particles.

2.2. Preparation of Doxycycline loaded BSA nanoparticles (DOX-BSA NPs)

Doxycycline hyclate (Sigma Aldrich, St. Louis, MO) loaded BSA nanoparticles were prepared using the procedure described above with modifications. Briefly, 25 mg of doxycycline hyclate (**DOX_{Tot}**) was dissolved along with 100 mg of BSA (**BSA_{Tot}**) in 2 mL of water and was allowed to stir at 500 rpm for 30 minutes. Following this, 4 mL of ethanol was added drop wise at a rate of 1 ml/min using an automated dispenser, which makes the solution turbid. To this 8% glutaraldehyde (40μg/mg BSA) was added to crosslink the albumin and the mixture was stirred for 2 hours at room temperature. The resulting solution was centrifuged at 14000 rpm for 10 mins to separate formed nanoparticles. Nanoparticles were washed thrice with DI water before proceeding with anti-elastin antibody conjugation as described previously [29]. The supernatant obtained from the washout was used to estimate the amount of free doxycycline (**DOX_F**) by measuring absorbance at 273 nm using a UV spectrophotometer (BioTek Instruments Inc., Winooski, VT). Difference between **DOX_{Tot}** and **DOX_F** gave the amount of doxycycline encapsulated (**DOX_{NP}**).

2.3. Characterization of DOX-BSA NPs

2.3.1. Size and zeta potential—The size and zeta potential of DOX-BSA NPs were measured using 90 Plus Particle Size Analyzer (Brookhaven Instruments Co, Holtsville, NY) with three runs performed per one sample batch (1 mg/mL solution). The size was also confirmed by scanning electron microscopy of nanoparticles.

2.3.2. Yield—5 mL of 1N NaOH was added to freshly prepared nanoparticles and stirred for 36 hrs to completely dissolve the bovine serum albumin. Then the absorbance of albumin was measured at 280 nm (A280) to calculate the amount of BSA present in the nanoparticles (**BSA_{NP}**). Nanoparticle yield fraction was calculated as total weight of BSA and doxycycline present in nanoparticles over initial amounts added.

$$\text{Yield} = [(\mathbf{BSA_{NP}} + \mathbf{DOX_{NP}})^{*}\mathbf{100}] / [\mathbf{BSA_{Tot}} + \mathbf{DOX_{Tot}}]$$

2.3.3. Loading—Percentage of loading of doxycycline in BSA nanoparticles is calculated using the following equation,

$$\text{Loading } \% = (\mathbf{DOX_{NP}}) / [\mathbf{Yield}^{*}(\mathbf{BSA_{Tot}} + \mathbf{DOX_{Tot}})]^{*}\mathbf{100}$$

2.3.4. *In vitro* release profile—Freshly prepared DOX-BSA NPs were re-suspended in 1 mL of DI water and incubated at 37°C. At specific time points, the nanoparticles were centrifuged and the supernatant was read at 273 nm to measure the amount of doxycycline released.

2.4. Cytotoxicity and nanoparticle uptake studies

Cytotoxicicy of DOX-BSA NPs at 0.5 mg/ml and 1 mg/ml concentrations was tested using the method described previously on rat lung fibroblasts, rat alveolar macrophages and human vascular endothelial cells (HuVECs) [30]. For nanoparticle uptake study two types of control NPs were used in addition to the normal NPs used for animal studies [30]. One batch was prepared with a positive surface charge (POS-DiR-BSA NPs) but same size, and one batch was prepared with smaller particle size (SM-DiR-BSA NPs) but with negative surface charge.

2.5. *In vivo* targeting study with DiR-BSA NPs

All animal studies performed according to the approved protocols and were compliant with the rules and regulations of Clemson University's Institutional Animal Care and Usage Committee (IACUC). To induce elastin damage and emphysema, we used one of the widely established elastase model of emphysema. Six week old male Sprague- Dawley (SD) rats (n=7) were used for *in vivo* targeting study. As shown in timeline graph (Fig 1), four of the rats were administered 50 U of porcine pancreatic elastase (PPE) via intra-tracheal instillation (**Elastase group**) (Elastin Products Company Inc., Owensville, MO) dissolved in 200 μl of PBS and filter sterilized. Remaining three rats received same volume of PBS as control (**Saline group**). The elastase treated rats developed elastin damage over four weeks. After 4 weeks, DiR loaded nanoparticles were injected intravenously through tail vein. Three each of elastase injected and control rats received DiR-BSA NPs conjugated with anti-elastin antibody (ELN-DiR-BSA NPs). One elastase injected rat received DiR-BSA NPs conjugated with anti-rat IgG (Sigma Aldrich, St. Louis, MO) as a control (IgG-DiR-BSA NPs). Twenty-four hours after injection, the rats were euthanized. Following euthanasia lung compliance was measured post-mortem, with the lungs *in situ*. Briefly, the trachea was cannulated and tied off with suture, a known volume of air was delivered to inflate the lung and the pressure change was recorded with the help of a transducer. Liver, heart, aorta, kidneys and spleen were harvested for measuring bio-distribution of DiR-BSA NPs.

2.6. Histological analysis

Processed tissue samples were embedded in paraffin and sections of 5 μm thick were made from the sagittal face. Hemotoxylin and eosin staining was used to observe general structural characteristics and enlargement of alveoli. Verhoff's Van Gieson (VVG) staining (Polysciences Inc., Warrinton, PA) was performed according to manufacturer's protocol to look at elastin damage in the alveolar walls of the tissue. Furthermore, perfusion fixed lungs were cut into small pieces and embedded in Richard-Allan Scientific™ Neg-50™ Frozen Section Medium (Thermo Scientific, Waltham, MA). 5 μm sections were made with a cryostat and observed using a CY-7 filter cube with EVOS® XL Cell Imaging System.

2.7. DiR signal measurement

After measuring compliance, lungs along with other harvested organs were imaged using IVIS® Lumina XR Imaging system (Caliper Life Sciences, Waltham, MA) set to excitation/emission of 745/790 nm, to observe bio-distribution of DiR-BSA NPs. Background signal was subtracted before analyzing the signal intensities from the organs. Bio-distribution of nanoparticles was calculated according to the equation below,

$$\text{Percentage Biodistribution} = \frac{\left(\frac{\text{Fluorescence in organ of interest}}{\text{Total fluorescence in all organs harveted}}\right)}{\text{Dry weight of organ of interest}} \times 100\%$$

Following this, the lungs were perfused with PBS and the resulting broncheoalveolar lavage fluid (BALF) was collected and frozen at −80°C until used. Then the lungs were perfusion fixed using 10% neutral buffered formalin (NBF) and stored for histological analysis along with other harvested organs.

2.8. *In vivo* Dox-BSA nanoparticle study

Six week old male Sprague-Dawley rats (n=10) were used for investigating the potential of doxycycline loaded nanoparticles in suppressing the MMP activity when administered systemically. As shown in timeline graph (Fig 1), all the rats received intra-tracheal instillation of PPE (50 U per animal). Three groups of animals were used to test the working of DOX-BSA NPs in comparison to the systemic injection of drug as an acute treatment option. Three rats did not receive any kind of treatment after elastase injection (**Non-treated group**); three rats received systemic injection of doxycycline hyclate solution via tail vein (300 μg per rat dissolved in 200 μl DI water) three days after the elastase administration and continued to receive weekly injections from then onwards (**Weekly IV group**). Four rats received one-time systemic injection of DOX-BSA NPs, conjugated with anti-elastin antibody, (10 mg/kg of animal) via tail vein only once i.e., three days after elastase administration (**DOX-BSA-NP group**). All the rats were euthanized after four weeks of treatment. After euthanasia, lungs of rats were cannulated and flushed with saline to obtain BALF.

2.9. Measurement of MMP activity in BALF

MMP activity in BALF was measured using internally quenched peptide substrates for MMPs 2&9 (Ex/Em= 280/360 nm, MMP Substrate III, Anaspec, CA) and MMP 12 (Ex/Em = 325/393 nm, 390 MMP FRET Substrate V, Anaspec, CA). One mg of the substrate was dissolved in 50 μL of DMSO, and the solution was diluted in 10 mL of development buffer (50 mM Tris Base, 5 mM $CaCl_2.2H_2O$, 200 mM NaCl, 0.02% brij 35). Substrate stock solution (2 μL) and 2 μL of the extracted protein were mixed with 96 μL of the development buffer and incubated for one hour at 37°C. A fluorescent plate reader was used to read endpoint florescence intensity.

2.10. *In situ* zymography

To examine activity of MMPs in the lung tissue samples *in situ* zymography on histological sections was performed as described before [30].

2.11. Statistical analysis

All *in vitro* experiments were done in triplicates. *In vitro* experiments were performed in triplicates and repeated twice; for *in vivo* studies, between three to four animals were used per group. Data were analyzed by one-way ANOVA followed by Dunnett's test. Levene's test was used to verify the homogeneity of variances. Dunnett's procedure was used when comparing all other treatments to a reference. The data are reported as the mean ± sstandard deviation. Results were considered to be significant with $p \leq 0.05$.

3. Results

3.1. DOX-BSA NPs characterization

We optimized drug loading, particle size, and charge by varying initial drug/polymer ratio, amount of glutaraldehyde used during nanoparticle preparation, stirring time, and solvent ratios (Table 1). Final chosen doxycycline loaded BSA NPs had an average size of 175±39.66 nm, which was confirmed by SEM (Fig 2A). Zeta potential of these particles was measured to be −59.8±4.67 mV. Total nanoparticle yield was 34.71±3.54 %. Loading percentage of doxycycline in NPs was 16.77±1.99%. Doxycycline from the nanoparticles was gradually released over a period of 28 days (Figure 2B). NPs released 9.68±3.4% drug at 24 hours and 13±4.56 % of the drug in 48 hours respectively. Amount of doxycycline released from BSA NPs steadily increased and reached 46.08±9.54 % in four weeks (Fig 2B). By this time the total amount of drug released was 3.97±0.59 mg.

3.2. Cytotoxicity and uptake of DOX-BSA NPs

3.2.1. *In vitro* cytotoxicity—DOX-BSA NPs tested at 0.5 mg/ml and 1 mg/ml concentrations were not found to be toxic in cell cultures of rat pulmonary fibroblasts, rat alveolar macrophages, or human vascular endothelial cells. Live dead assay of all the three types of cells showed no abnormalities in morphology and no dead cells. The cell viability was similar to the control group. On the other hand, ethanol treatment (positive control) lead to dying of all cells (Fig 3A).

3.2.2. Nanoparticle uptake—DiR-BSA NPs as prepared for *in vivo* studies showed no uptake by endothelial cells, pulmonary interstitium by fibroblasts, and alveolar macrophages in cell cultures due to their negative surface charge and size. When surface charge was changed to positive by adding chitosan on the surface (POS-DiR-BSA) or size was reduced but surface charge was kept negative (SM-DiR-BSA), we found these NPs were taken up by all the cells (Fig 3B) clearly showing that suface negative charge and size is important for avoiding cellular uptake.

3.3. Elastase model and *in vivo* targeting study

No severe damage and unexpected mortality were observed due to the intra-tracheal instillation of 50 U of PPE to the rats. The Elastase group rats did not show any signs of increased lung compliance and labored breathing. Compliance of the lungs measured were not statistically different between Saline and Elastase groups (0.334 ± 0.074 vs 0.372 ± 0.062 ml/cm H_2O; p=0.29). This shows that the elastase concentration chosen caused only mild emphysema in the lungs.

3.4. Histological Analysis

The damage in lungs was confirmed using H&E staining of histological sections. H&E stain showed areas of air space enlargement in the elastase group rats (Figure 4A and 4B). VVG staining for elastin revealed damaged elastin in the alveolar walls which could be seen as faded black fibers (Figure 4C–4F).

3.5. DiR signal measurement

DiR-BSA NPs when delivered systemically and allowed to circulate for 24 hours, showed specific targeting to damaged elastin in lungs (Figure 5A). Saline group rats, which received PBS instillation showed negligible signal of NPs in their lungs (Fig 5A). Aorta, which also has healthy elastin did not have any signal from the NPs in both groups (Fig 5B), clearly suggesting that NPs target only degraded elastin in lungs. Frozen sections of the lung from elastase treated group showed nanoparticles in the lungs of elastase group associated with elastin (Fig 5C and 5D). Targeting percentage for was calculated by normalizing the epifluorescence signal to average dry weight of the organ. Compared to control group, Elastase group lungs showed five times higher signal (0.74±0.48 % vs 4.36±2.18 %) (Fig 5E). Rest of the NPs were found in liver, spleen, and kidneys while heart showed no signal in both groups (Figure 5F).

3.6. Measurement of MMP activity in BALF

As DiR dye loaded NPs showed good targeting to damaged elastin in lungs, we next tested if nanoparticles loaded with doxycycline, a broad spectrum MMP inhibitor, can be delivered to the lungs and be effective in preventing MMP activity. MMP activity in the BALF was measured using specific FRET substrates for MMPs 2, 9 and 12. Non-treated group and Weekly IV group rats showed high MMP activity. Weekly IV group rats showed slight decrease in MMP activity compared to the Non-treated group but this was not statistically significant. It suggested that weekly drug injections were ineffective in inhibiting MMPs in lungs. When DOX-BSA NPs were delivered systemically only once at day 3, lungs showed significantly less MMP activity even after four weeks (Fig 6A). Using one way ANOVA ($p<0.05$) and Dunnett's test for multiple comparisons, it was found that DOX-BSA-NP group had significantly lower MMP 2, 9 and 12 activity compared to Non-treated group and Weekly IV group was found not to be different from Non-treated group.

3.7. *In situ* zymography

In situ zymography is used to detect active MMPs in histological sections. When the intensity of fluorescence was compared between Weekly IV and DOX-BSA-NP groups, we observed a significant suppression of signal from DOX-BSA-NP group's lung section compared to the IV drug injection (Fig 6B). This reduced MMP activity concurred with the FRET assay results showing that one nanoparticle injection can suppress MMP activity for an extended period of time.

Discussion

The present study shows a novel targeting strategy for delivering drugs to emphysematous lungs using anti-elastin coated BSA nanoparticles. It also shows that such targeted

nanoparticles loaded with doxycycline hyclate can suppress MMP activity in the lungs for prolonged periods.

Emphysema is responsible for damage of alveoli owing to the chronic inflammation in the lungs there by decreasing gas exchange capability of lungs. It also leads to the loss of elastin fibers that results in loss of elastic recoil of lungs making the alveoli collapse during breath exhalation requiring the patient to use greater force to exhale the air out. Most of the available treatments provide relief to the patients by bronchodilation; however, new anti-inflammatory agents are being developed [31]. The most general route of administration of drugs for pulmonary applications is by inhalation. There are many advantages of this route like local delivery, availability of drug, needleless treatment but at the same time, it may not be suitable for people with diseases like emphysema. It has been shown that inspirational capacity of COPD patients is less than that of normal subjects, which might reduce drug deposition [32, 33]. Apart from size hydrophilicity/hydrophobicity of the drug, mucociliary clearance mechanisms, drug metabolism in lungs can dictate what happens to the inhaled drug. Inhaled drug particles also have to survive phagocytosis by alveolar macrophages. One recent study has shown that, while modeling lobar distribution of particles, differences do exist between normal and emphysematous mice with factors like airway collapse, smaller airways, particle transport through expiration may impact particle deposition [34]. Thus, targeting lungs via a systemic route like intravenous administration of nanoparticles seems promising. Elastin damage is one of the characteristics observed at the extracellular matrix level in emphysema. Matured elastic fibers have amorphous elastin protein wrapped around by microfibrils and other proteins [35, 36]. During inflammation, MMPs can degrade these outer microfibrils and expose core elastin to elastases [37–39]. We took advantage of this distinction to target NPs tissues that experience elastic fiber degradation as a part of their pathophysiology.

After several parameter optimizations as shown in Table 1, we obtained ~200 nm size particles with negative surface charge and good drug loading. We have shown earlier that this size and negative surface charge and surface conjugation of elastin antibody allowed NPs to target degraded elastin in arteries in experimentally created aneurysms and vascular calcification in rats [29, 30, 40]. We wanted to extend these studies to lungs. The nanoparticles possessed required surface charge and size to not being phagocytosed by macrophages. They were also PEGylated to increase their circulation time in the body. Our nanoparticle uptake study results coincide with the observed fact that particles less than 0.26 microns can escape phagocytosis by macrophages [41].

The size and negative surface charge of these nanoparticles are needed to avoid uptake and phagocytosis by macrophages and by other cells like fibroblasts and endothelial cells *in vivo*. We show that surface negative chage and size of ~200 nm prevented cellular uptake of DOX loaded NPs. This was desirable as we wanted nanoparticles to be bound to degraded elastin in the extracellular space and not cleared right away by phagocytosis. When surface charge was changed to positive (POS-DiR-BSA) or NPs were made smaller in size (SM-DiR-BSA NPs), we found that these were readily phagocytosed by alveolar macrophages *in vitro*. This result was important in the sense that phagocytosis by alveolar macrophages is one of the clearance mechanisms adopted by the lungs to get rid of foreign particles.

We used elastase instillation rat model of emphysema, which causes elastin damage and air space enlargement in lungs [42]. VVG staining showed faded black fibers along the alveolar walls in elastase treated rats showing degradation of elastin. Thus, this model was an ideal test bed for us to validate our nanoparticle targeting and inhibiting MMPs in lungs. The strong DiR signal from elastase damaged lungs combined with the observation of aortae in the same rats being void of signal proved that the nanoparticles target only damaged elastin in lungs. Elastase instilled rats which received IgG-DiR-BSA NPs showed no targeting, which proved that elastin antibody coating was pre-requisite for targeting (data not shown).

We did not observe any significant changes in the lung compliance between the saline and elastase groups as we expected to only see a mild emphysema with our treatment. We believe that this might be because of the low dosage that has been administered to the rats (50 U per animal). Another reason is likely a result of the intra-tracheal delivery method of the protease (inhaled delivery may produce more uniform damage, but carries its own problems). But we know and have demonstrated that septal disruption occurred, making the lung a viable emphysema model for the study aims.

We observed ~5-fold increase in NP targeting for elastin antibody coated NPs when compared to the Saline group. Very few studies have shown lung specific targeting of nanoparticles. Documented results show much variation in the percentage of particles reaching lungs. Bazile et al. used ^{14}C-polylactic acid (PLA) nanoparticles coated with human serum albumin (HSA) and showed a passive targeting percentage of 0.09% and 0.01% at days 1 and 7 respectively [43]. Akasaka et al [44] have seen only slight localization of BSA nanoparticles coated with lung carcinoma monoclonal antibodies (mAbs) to Lewis lung carcinoma in mice lungs. This is the only study that has shown targeting with antibody-coated nanoparticles used for targeted delivery of drugs to lungs. We have shown that our nanoparticles exhibit specific targeting with higher percentage of particles going to lungs compared to documented results. Overall, our strategy of targeting degraded elastin was specific to damaged areas of lungs only and would provide drug release where it is needed most.

Matrix metalloproteinases, especially MMP 12, play a central role in extracellular matrix degradation and progression of emphysema [45, 46] and their inhibition has shown protection against emphysema development in animal models [47, 48]. Churg et al. further stressed the importance of MMP-12 in cigarette smoke model of emphysema by showing reduced levels of this protein produced by alveolar macrophages when treated with α-1 anti-trypsin [49].

Our aim was to deliver a broad-spectrum MMP inhibitor like doxycycline, encapsulated in a biodegradable nanoparticle system, to mitigate MMP activity. Doxycycline is a potent inhibitor of MMPs especially MMP-8 and -9 [50–52]. Doxycycline has been previously shown to reduce the severity of abdominal aortic aneurysms (AAAs) in various animal models. Manning et al., [53] have shown reduction of AAA formation in Ang II murine model of the disease. Their study results also coincide with Uitto et al., [54] who also report decreased MMP2 activity and also decreased MMP2 gene expression in epithelial cell cultures. Petrinec et al., [55] have observed decreased local MMP9 production in the

abdominal aorta which led to the preservation of elastic matrix in the rats treated with doxycycline injections daily.

Broncheoalveolar lavage fluid (BALF) is a key indicator of inflammation that is going on in lungs. Measurement of MMP activity from BALF evaluated the efficacy of nanoparticles in delivering functional doxycycline to the lungs. Non-treated rats without any drug treatment showed high MMP activity in BALF. This level of activity was similar to rats receiving weekly injections of doxycycline, clearly showing drug alone was inefficient in inhibiting lung MMPs. We show that targeting of nanoparticles to damaged elastin in the lungs and a controlled release of doxycycline played an important role in keeping down the MMP activity levels in rats that received single DOX-BSA NPs injection. An obvious advantage of such treatment is requirement of lower dosages.

Dalvi et al., [56] have reported significant improvement in lung functions when moderate to severe COPD patients were treated with doxycycline (100 mg per day). In another recent pilot study Bhattacharya et al., [57] have observed pulmonary function improvements with doxycycline treatment (100 mg per day) compared to standard pharmacotherapy. In animal models, Rossiter et al., [58] have showed VEGF*LoxP* mice instilled through the trachea with an adeno-associated virus expressing Cre recombinase had reduced mean linear intercept (MLI) values with continuous doxycycline treatment along with reduction in MMPs. Sochor et al., [59] have demonstrated MMP-9 inhibition and thus pancreatitis-associated lung injury in rats with doxycycline treatment (30 mg/kg). Doroszko et al., [60] have reported MMP-9 inhibition by doxycycline (2 mg/kg) in mechanical ventilation-induced lung injury in Wistar rats. These experiments lasted for less than one day. On a similar scale, the average amount doxycycline released into the body of each rat in 24 hours is 0.163 mg/kg in our current study. This corresponds up to ~180 and ~12 fold decrease in the amount of drug required for MMP inhibition with targeted delivery compared to Sochor et al., and Doroszko et al., results respectively. Doxycycline is used as an example in this paper to pave the way for many other drugs that can be targeted to lungs by our novel NPs. The reduced dosage using targeted delivery can be particularly useful when toxic drugs have to be delivered for treatment of diseases like lung cancers.

Conclusion

In conclusion, by taking advantage of elastin damage that occurs in emphysema as a part of its pathological process, we have developed a novel bio-degradable polymeric nanoparticle system that targets to lungs. We have confirmed the targeting specificity of these particles. Doxycycline loaded BSA NPs were optimized in their size, surface properties, yield, drug loading and release properties. Targeted single dose delivery of doxycycline nanoparticles have led to significant inhibition of MMPs in the lungs for up to 4 weeks *in vivo*. This opens up a promising way of controlling inflammation in emphysema there by stopping further damage to the lungs.

Acknowledgments

We gratefully acknowledge funding from the NIH grant P20GM103444 and the Hunter Endowment to NRV.

References

1. Tuder RM, et al. State of the art. Cellular and molecular mechanisms of alveolar destruction in emphysema: an evolutionary perspective. Proc Am Thorac Soc. 2006; 3(6):503–510. [PubMed: 16921129]
2. Taraseviciene-Stewart L, Voelkel NF. Molecular pathogenesis of emphysema. J Clin Invest. 2008; 118(2):394–402. [PubMed: 18246188]
3. Sharafkhaneh A, Hanania NA, Kim V. Pathogenesis of emphysema: from the bench to the bedside. Proc Am Thorac Soc. 2008; 5(4):475–477. [PubMed: 18453358]
4. Chrzanowski P, et al. Elastin content of normal and emphysematous lung parenchyma. Am J Med. 1980; 69(3):351–359. [PubMed: 7416182]
5. Cardoso WV, et al. Collagen and elastin in human pulmonary emphysema. Am Rev Respir Dis. 1993; 147(4):975–981. [PubMed: 8466136]
6. Black PN, et al. Changes in elastic fibres in the small airways and alveoli in COPD. Eur Respir J. 2008; 31(5):998–1004. [PubMed: 18216063]
7. Barnes PJ. Chronic obstructive pulmonary disease * 12: New treatments for COPD. Thorax. 2003; 58(9):803–808. [PubMed: 12947145]
8. Ngkelo A, Adcock IM. New treatments for COPD. Curr Opin Pharmacol. 2013; 13(3):362–369. [PubMed: 23602653]
9. Dunsmore SE. Treatment of COPD: a matrix perspective. Int J Chron Obstruct Pulmon Dis. 2008; 3(1):113–122. [PubMed: 18488434]
10. Barnes, P. Anti-Inflammatory Therapeutics in COPD: Past, Present, and Future. In: Rogers, TJ.; Criner, GJ.; Cornwell, WD., editors. Smoking and Lung Inflammation. New York: Springer; 2013. p. 191-213.
11. Barnes PJ. Inhaled corticosteroids in COPD: a controversy. Respiration. 2010; 80(2):89–95. [PubMed: 20501985]
12. Churg A, Zhou S, Wright JL. Series "Matrix Metalloproteinases in Lung Health and Disease" Matrix Metalloproteinases in Copd. European Respiratory Journal. 2012; 39(1):197–209. [PubMed: 21920892]
13. Pemberton PA, et al. An inhaled matrix metalloprotease inhibitor prevents cigarette smoke-induced emphysema in the mouse. Copd. 2005; 2(3):303–310. [PubMed: 17146995]
14. Selman M, et al. Matrix metalloproteinases inhibition attenuates tobacco smoke-induced emphysema in guinea pigs. Chest. 2003; 123(5):1633–1641. [PubMed: 12740284]
15. Neidich JA. Inborn Errors of Development: The Molecular Basis of Clinical Disorders of Morphogenesis. American Journal of Human Genetics. 2005; 76(2):368–368.
16. Fujita M, et al. Doxycycline attenuated lung injury by its biological effect apart from its antimicrobial function. Pulm Pharmacol Ther. 2007; 20(6):669–675. [PubMed: 17045828]
17. Fujita M, et al. Doxycycline attenuated pulmonary fibrosis induced by bleomycin in mice. Antimicrob Agents Chemother. 2006; 50(2):739–743. [PubMed: 16436734]
18. Liu J, et al. Mechanism of inhibition of matrix metalloproteinase-2 expression by doxycycline in human aortic smooth muscle cells. J Vasc Surg. 2003; 38(6):1376–1383. [PubMed: 14681644]
19. Sivaraman B, Ramamurthi A. Multifunctional nanoparticles for doxycycline delivery towards localized elastic matrix stabilization and regenerative repair. Acta Biomater. 2013; 9(5):6511–6525. [PubMed: 23376127]
20. Griffin MO, et al. Tetracyclines: a pleitropic family of compounds with promising therapeutic properties. Review of the literature. Am J Physiol Cell Physiol. 2010; 299(3):C539–C548. [PubMed: 20592239]
21. Guillermo Moñux, D., et al. Actual Pharmacological Treatment to Reduce Growth of Small Abdominal Aneurysm. INTECH Open Access Publisher; 2011.
22. Watts, A.; Williams, R, III. Nanoparticles for Pulmonary Delivery. In: Smyth, HDC.; Hickey, AJ., editors. Controlled Pulmonary Drug Delivery. New York: Springer; 2011. p. 335-366.
23. Pathak Y, Benita S. Antibody-mediated drug delivery systems : concepts, technology, and applications. 2012

24. Azarmi S, Roa WH, Lobenberg R. Targeted delivery of nanoparticles for the treatment of lung diseases. Adv Drug Deliv Rev. 2008; 60(8):863–875. [PubMed: 18308418]
25. Byron PR, Patton JS. Drug delivery via the respiratory tract. J Aerosol Med. 1994; 7(1):49–75. [PubMed: 10147058]
26. Newman SP, et al. Effects of various inhalation modes on the deposition of radioactive pressurized aerosols. Eur J Respir Dis Suppl. 1982; 119:57–65. [PubMed: 6807705]
27. Vincent JH, et al. Kinetics of deposition and clearance of inhaled mineral dusts during chronic exposure. Br J Ind Med. 1985; 42(10):707–715. [PubMed: 2864076]
28. Elzoghby AO, Samy WM, Elgindy NA. Albumin-based nanoparticles as potential controlled release drug delivery systems. J Control Release. 2012; 157(2):168–182. [PubMed: 21839127]
29. Lei Y, Nosoudi N, Vyavahare N. Targeted chelation therapy with EDTA-loaded albumin nanoparticles regresses arterial calcification without causing systemic side effects. Journal of Controlled Release. 2014; 196:79–86. [PubMed: 25285609]
30. Nosoudi N, et al. Prevention of abdominal aortic aneurysm progression by targeted inhibition of matrix metalloproteinase activity with batimastat-loaded nanoparticles. Circ Res. 2015; 117(11):e80–e89. [PubMed: 26443597]
31. Loukides S, et al. Novel anti-inflammatory agents in COPD: targeting lung and systemic inflammation. Curr Drug Targets. 2013; 14(2):235–245. [PubMed: 23256720]
32. Azouz W, et al. The inhalation characteristics of patients when they use different dry powder inhalers. J Aerosol Med Pulm Drug Deliv. 2015; 28(1):35–42. [PubMed: 24815999]
33. Azouz W, et al. Inhalation characteristics of asthma patients, COPD patients and healthy volunteers with the Spiromax(R) and Turbuhaler(R) devices: a randomised, cross-over study. BMC Pulm Med. 2015; 15:47. [PubMed: 25927483]
34. Oakes JM, et al. Distribution of aerosolized particles in healthy and emphysematous rat lungs: comparison between experimental and numerical studies. J Biomech. 2015; 48(6):1147–1157. [PubMed: 25682537]
35. Rosenbloom J, Abrams WR, Mecham R. Extracellular matrix 4: the elastic fiber. FASEB J. 1993; 7(13):1208–1218. [PubMed: 8405806]
36. Sakai LY, Keene DR, Engvall E. Fibrillin, a new 350-kD glycoprotein, is a component of extracellular microfibrils. J Cell Biol. 1986; 103(6 Pt 1):2499–2509. [PubMed: 3536967]
37. Ashworth JL, et al. Fibrillin degradation by matrix metalloproteinases: implications for connective tissue remodelling. Biochem J. 1999; 340(Pt 1):171–181. [PubMed: 10229672]
38. Fukuda Y, Ferrans VJ. Pulmonary elastic fiber degradation in paraquat toxicity. An electron microscopic immunohistochemical study. J Submicrosc Cytol Pathol. 1988; 20(1):15–23. [PubMed: 3370614]
39. McLaughlin PJ, et al. Targeted disruption of fibulin-4 abolishes elastogenesis and causes perinatal lethality in mice. Mol Cell Biol. 2006; 26(5):1700–1709. [PubMed: 16478991]
40. Sinha A, et al. Nanoparticle targeting to diseased vasculature for imaging and therapy. Nanomedicine: Nanotechnology, Biology and Medicine. 10(5):e1003–e1012.
41. Lauweryns JM, Baert JH. Alveolar clearance and the role of the pulmonary lymphatics. Am Rev Respir Dis. 1977; 115(4):625–683. [PubMed: 322558]
42. Antunes MA, Rocco PR. Elastase-induced pulmonary emphysema: insights from experimental models. An Acad Bras Cienc. 2011; 83(4):1385–1396. [PubMed: 22159348]
43. Bazile DV, et al. Body distribution of fully biodegradable [14C]-poly(lactic acid) nanoparticles coated with albumin after parenteral administration to rats. Biomaterials. 1992; 13(15):1093–1102. [PubMed: 1493193]
44. Akasaka Y, et al. Preparation and evaluation of bovine serum albumin nanospheres coated with monoclonal antibodies. Drug Des Deliv. 1988; 3(1):85–97. [PubMed: 3255326]
45. Lagente V, et al. Role of matrix metalloproteinases in the development of airway inflammation and remodeling. Braz J Med Biol Res. 2005; 38(10):1521–1530. [PubMed: 16172745]
46. Demedts IK, et al. Elevated MMP-12 protein levels in induced sputum from patients with COPD. Thorax. 2006; 61(3):196–201. [PubMed: 16308335]

47. Churg A, et al. Effect of an MMP-9/MMP-12 inhibitor on smoke-induced emphysema and airway remodelling in guinea pigs. Thorax. 2007; 62(8):706–713. [PubMed: 17311841]
48. Vandenbroucke RE, Dejonckheere E, Libert C. A therapeutic role for matrix metalloproteinase inhibitors in lung diseases? Eur Respir J. 2011; 38(5):1200–1214. [PubMed: 21659416]
49. Churg A, et al. Alpha1-antitrypsin suppresses TNF-alpha and MMP-12 production by cigarette smoke-stimulated macrophages. Am J Respir Cell Mol Biol. 2007; 37(2):144–151. [PubMed: 17395890]
50. Suomalainen K, et al. Specificity of the anticollagenase action of tetracyclines: relevance to their anti-inflammatory potential. Antimicrob Agents Chemother. 1992; 36(1):227–229. [PubMed: 1317148]
51. Fiotti N, et al. Short term effects of doxycycline on matrix metalloproteinases 2 and 9. Cardiovasc Drugs Ther. 2009; 23(2):153–159. [PubMed: 19052856]
52. Zhao S, et al. Effects of doxycycline on serum and endometrial levels of MMP-2, MMP-9 and TIMP-1 in women using a levonorgestrel-releasing subcutaneous implant. Contraception. 2009; 79(6):469–478. [PubMed: 19442784]
53. Manning MW, Cassis LA, Daugherty A. Differential effects of doxycycline, a broad-spectrum matrix metalloproteinase inhibitor, on angiotensin II-induced atherosclerosis and abdominal aortic aneurysms. Arterioscler Thromb Vasc Biol. 2003; 23(3):483–488. [PubMed: 12615694]
54. Uitto VJ, et al. Doxycycline and chemically modified tetracyclines inhibit gelatinase A (MMP-2) gene expression in human skin keratinocytes. Ann N Y Acad Sci. 1994; 732:140–151. [PubMed: 7978787]
55. Petrinec D, et al. Doxycycline inhibition of aneurysmal degeneration in an elastase-induced rat model of abdominal aortic aneurysm: preservation of aortic elastin associated with suppressed production of 92 kD gelatinase. J Vasc Surg. 1996; 23(2):336–346. [PubMed: 8637112]
56. Dalvi PS, et al. Effect of doxycycline in patients of moderate to severe chronic obstructive pulmonary disease with stable symptoms. Ann Thorac Med. 2011; 6(4):221–226. [PubMed: 21977068]
57. Bhattacharyya P, et al. Long-term doxycycline and lung function in chronic obstructive pulmonary disease: A pilot observation. Lung India. 2014; 31(3):306–307. [PubMed: 25125830]
58. Rossiter HB, et al. Doxycycline treatment prevents alveolar destruction in VEGF-deficient mouse lung. J Cell Biochem. 2008; 104(2):525–535. [PubMed: 18181212]
59. Sochor M, et al. Inhibition of matrix metalloproteinase-9 with doxycycline reduces pancreatitis-associated lung injury. Digestion. 2009; 80(2):65–73. [PubMed: 19494493]
60. Doroszko A, et al. Effects of MMP-9 inhibition by doxycycline on proteome of lungs in high tidal volume mechanical ventilation-induced acute lung injury. Proteome Sci. 2010; 8:3. [PubMed: 20205825]

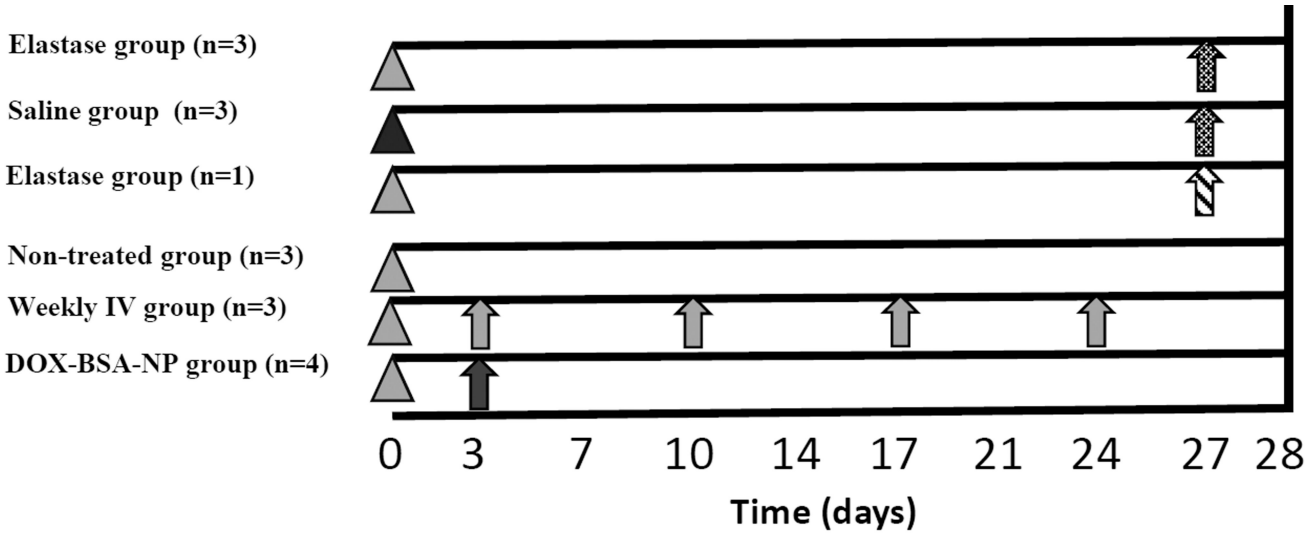

intra-tracheal elastase instillation

intra-tracheal saline instillation

ELN-DiR-BSA NPs-tail vein

IgG-DiR-BSA NPs-tail vein

Doxycycline IV injection

DOX-BSA NPs-tail vein

ELN-DiR-BSA NPs : DiR loaded BSA nanoparticles conjugated with anti-elastin antibody
IgG-DiR-BSA NPs : DiR loaded BSA nanoparticles conjugated with IgG antibody
IV group : intravenous injection of doxycycline
DOX-BSA-NPs : Doxycycline loaded BSA nanoparticles conjugated with anti-elastin antibody

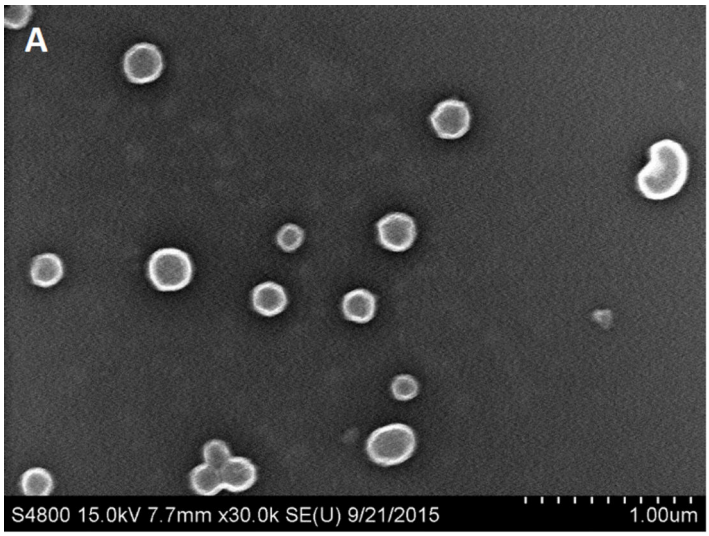

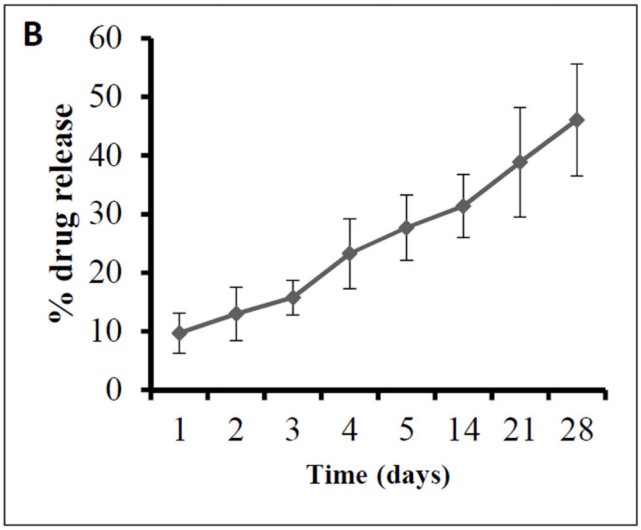

Particle size: 175±39.66 nm;
Zeta Potential: 59.8±4.67 mV;
Yield percentage: 34.71±3.54 %;

Drug loading: 16.77±1.99 %

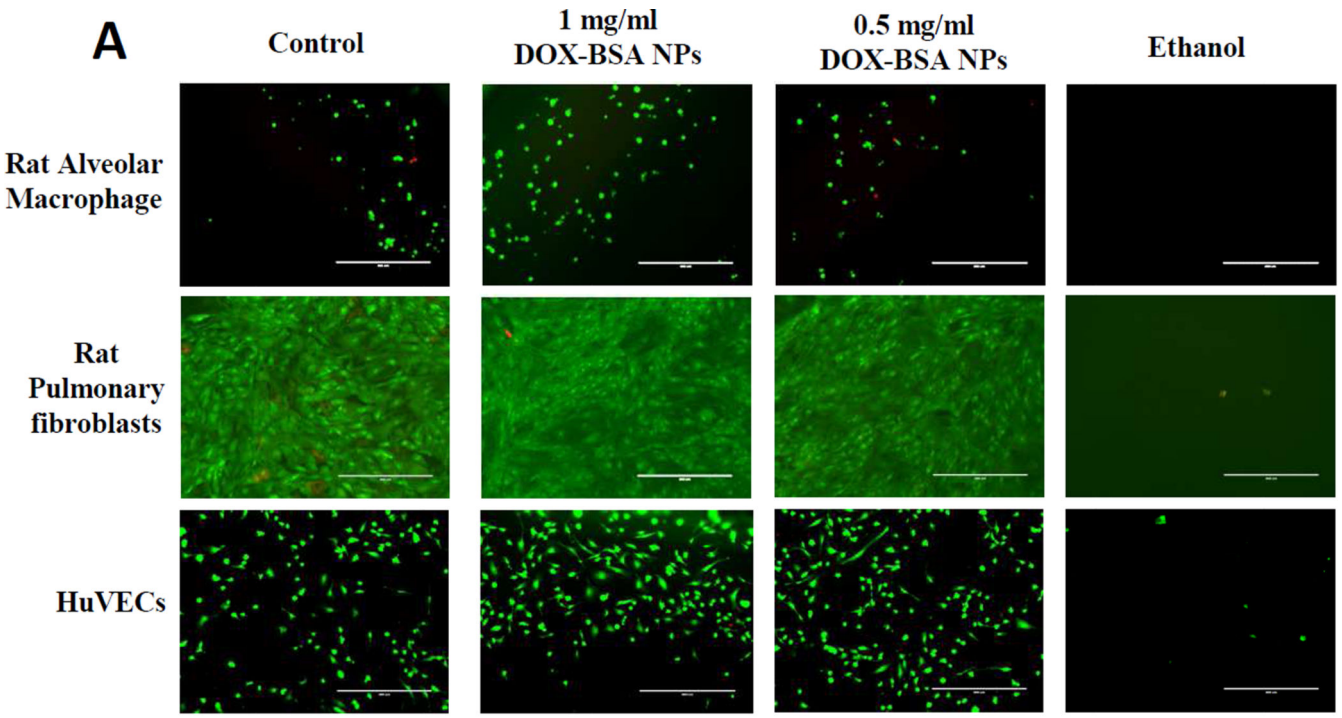

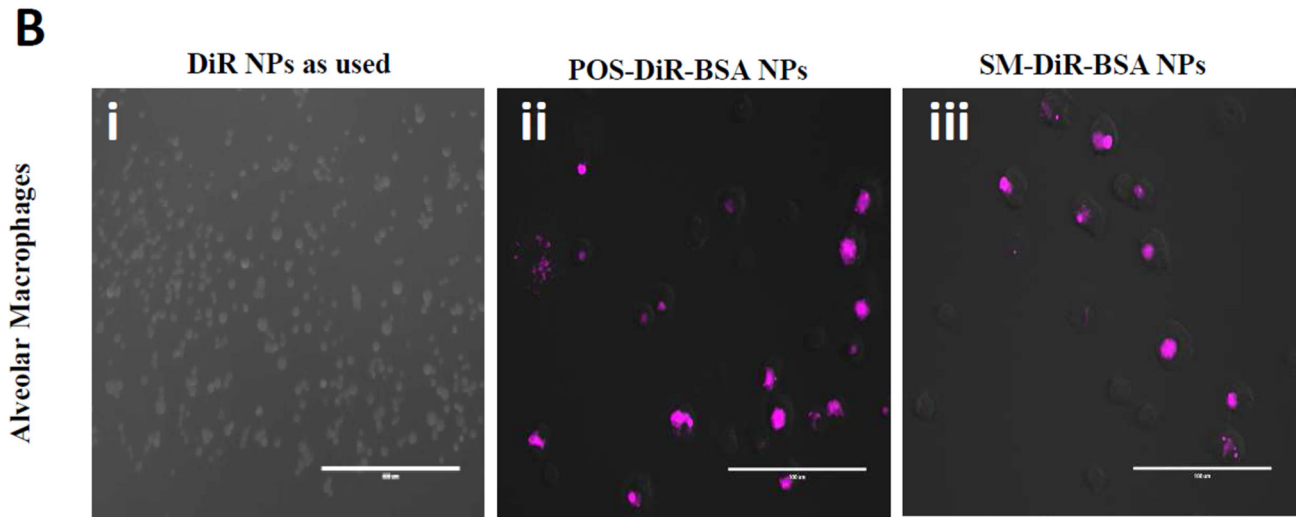

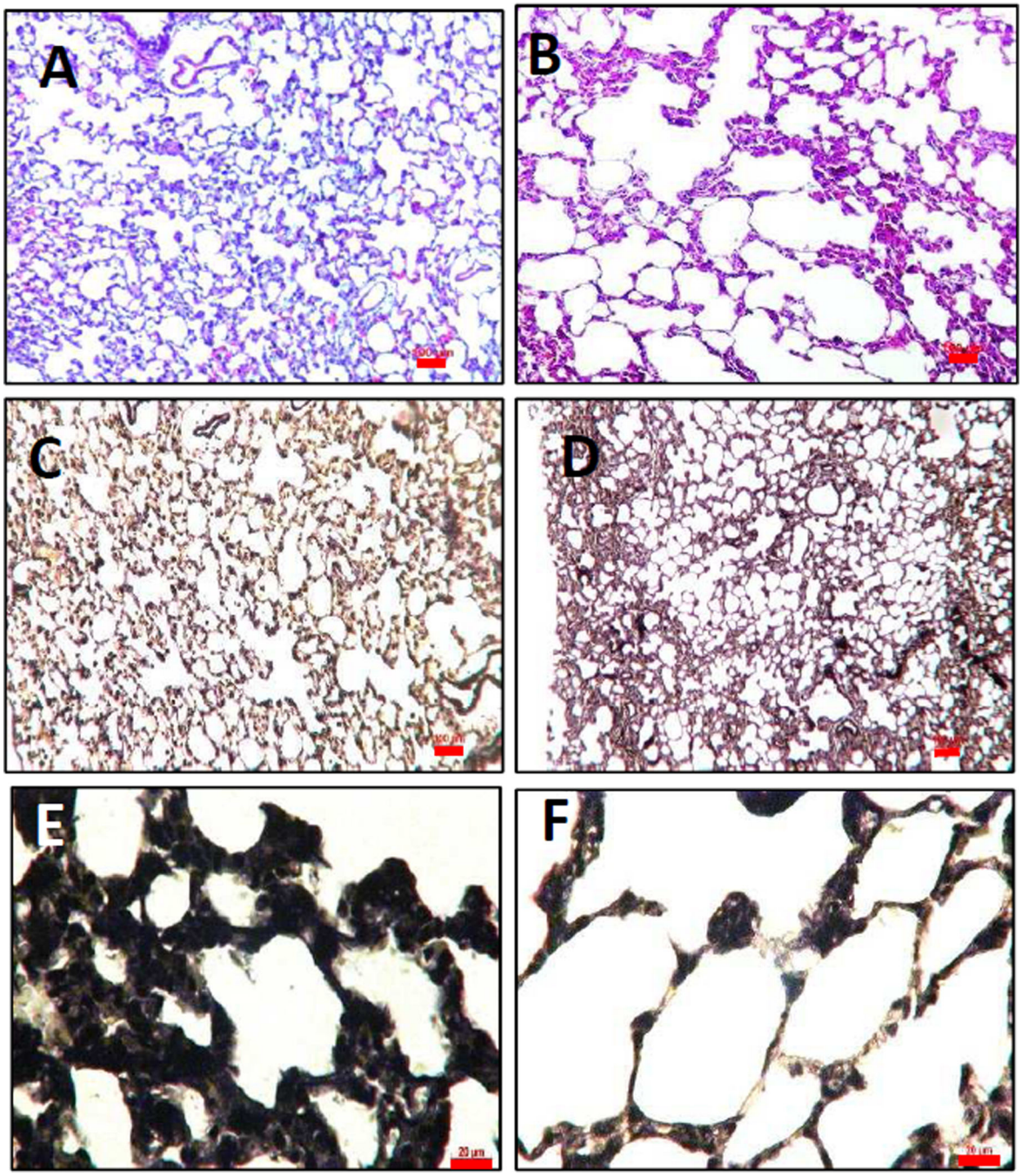

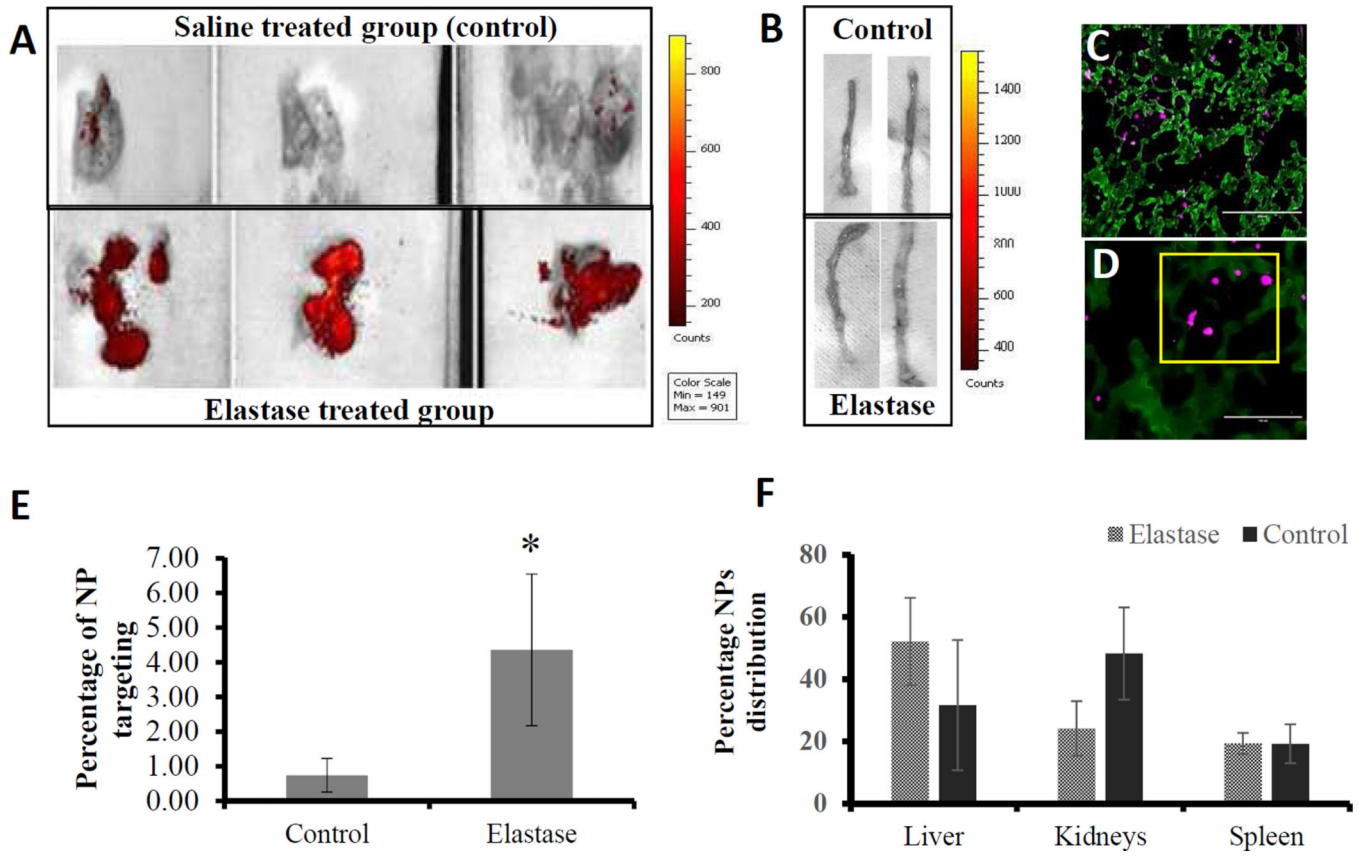

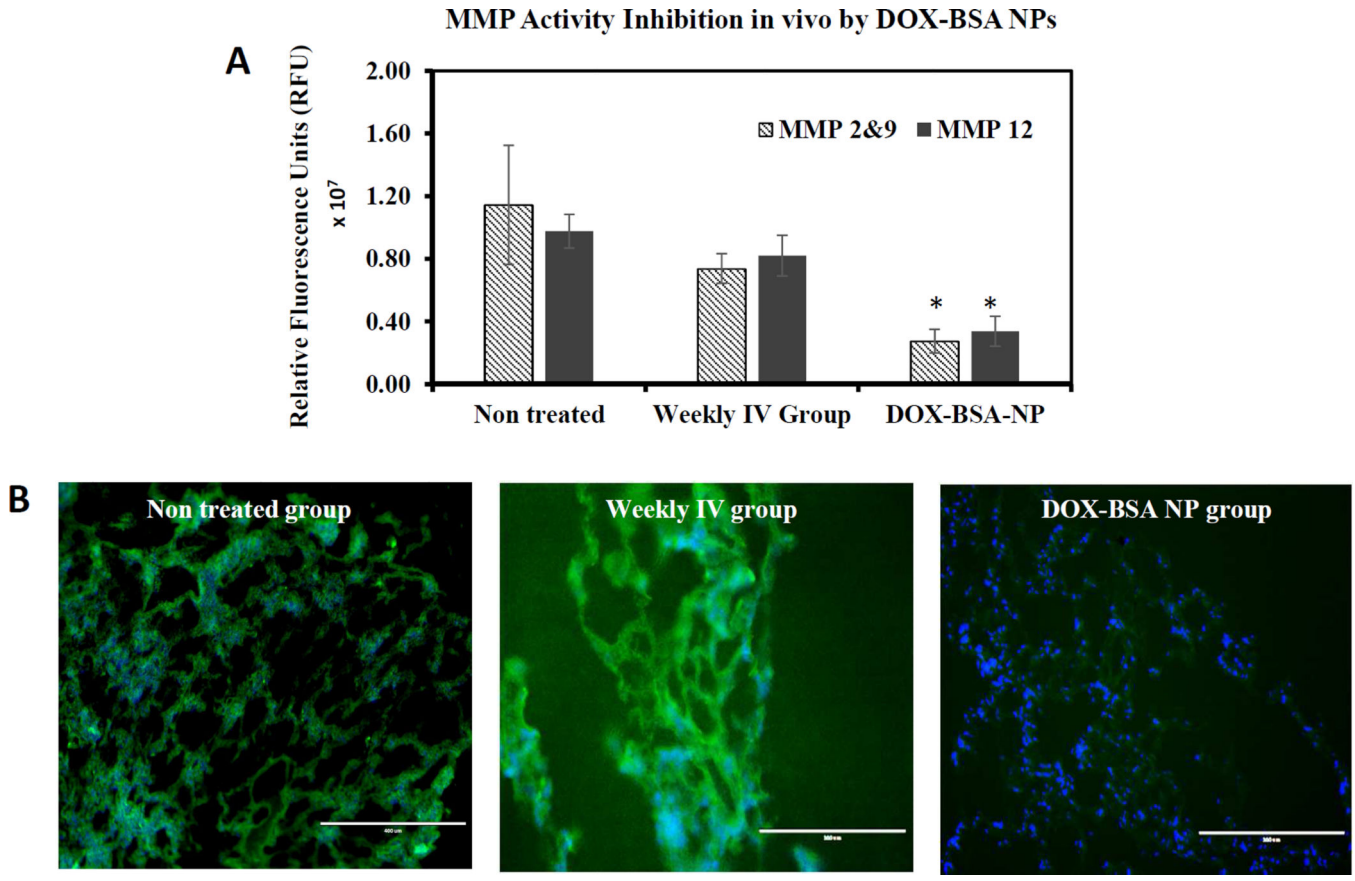

Table 1

Optimization of Doxycycline nanoparticles

	Lot #1	Lot #2	Lot #3	Lot #4	Lot #5
Drug to Polymer ratio	1:10 (Doxycycline Monohydrate)	1:5 (Doxycycline Monohydrate)	1:4 (Doxycycline Monohydrate)	1:4 (Doxycycline Hyclate)	1:4 (Doxycycline Hyclate)
Gluteraldehyde (μg/mg BSA)	42	Half during stirring and half during sonication	42	46.8	40
Stirring time	60	30	60	30	30
Desolvant to solvent ratio	6	6	6	2	2
Sonication time (min)	60	60	60	30, 60, 90	120 (stirring instead of sonication)
Results/ comments	Negligible loading of drug. No nanoparticles formed	No nanoparticles formed.	Loading was 6.77±1.7 % Particle size was ~608 nm	Particle sizes were ~458 nm, ~469 nm and ~390 nm for respective sonication times.	Particle size was in the range of 170–200 nm. Zeta potential was −60 mV. Loading was 16.77±1.99 %